STRUCTURAL CONTROL AND HEALTH MONITORING
Struct. Control Health Monit. 2006; **13**:132–146
Published online 19 December 2005 in Wiley InterScience (www.interscience.wiley.com). DOI: 10.1002/stc.141

Structural health monitoring by Lyapunov exponents of non-linear time series

Fabio Casciati*,† and Sara Casciati

Department of Structural Mechanics, University of Pavia, via Ferrata 1, Pavia I 27100, Italy

SUMMARY

In this study, structural health monitoring is pursued by collecting multi-channel measurements and by computing, directly from them, the Lyapunov exponents. The latter quantities are invariants of the dynamic system, so that their different values, associated with different time histories obtained from the same structure, denote damage. First, the problem is framed in the general theory. The structural health monitoring strategy is then formulated, with special care being devoted to its capability of localizing damage. The procedure is finally validated by using the time histories which were collected during the experimental tests on the model of a monumental arch. Copyright © 2005 John Wiley & Sons, Ltd.

KEY WORDS: dynamic system; Kolmogorov entropy; Lyapunov dimension; Lyapunov exponents; observed variables space; structural health monitoring

1. INTRODUCTION

The evolution in time of a dynamic system is defined in a state-space, and it is uniquely characterized when h independent variables are simultaneously specified. In other words, one could say that the dynamics lives in an h-dimensional manifold, which is likely to be curved. The embedding of such a curved manifold into a Cartesian space, R^l, with l denoting the state-space dimension, is ruled by the Whitney theorem and by its extension to fractal environments [1], which ensures that $l = 2h + 1$, where time is one of the variables. The other components of a dynamic problem are the initial conditions, to which the chaotic systems are sensitive [2], and the presence of stochastic components. As stated in Reference [1], 'successful approaches either assume the non-linearity to be a small perturbation of an essentially linear stochastic process, or they regard the stochastic element as a small contamination of an essentially deterministic, non-linear process'.

*Correspondence to: F. Casciati, Department of Structural Mechanics, University of Pavia, via Ferrata 1, I 27100 Pavia, Italy.
†E-mail: fabio@dipmec.unipv.it

Contract/grant sponsor: Italian Ministry of Instruction, University and Research (MIUR); contract/grant number: PRIN04

Received 30 May 2005
Revised 6 September 2005

Structural health monitoring (SHM) is usually pursued by a comparison of the models inferred from the time histories of some measured quantities, which are collected during subsequent time intervals of the system lifetime. Actually, the knowledge of the entire dynamic system is not required, since the different damage detection algorithms usually rely on different model invariants, such as eigenvalues or wavelet spectra [3–5].

The comparison of models built directly from the monitored time histories, rather than of the previously defined dynamic system models, was recently investigated by the second author in References [6, 7]. Such an approach is based on the following assumptions [1]:

(1) The measurements are reproducible. Reproducibility is closely connected to stationarity, in both its two following aspects: the parameters of the studied systems are constant during the measurement period, and an asymptotic stationarity results from infinitely long observation times (despite the signals non-stationarity in a single time window, as it usually occurs in the presence of intermittency).
(2) The resulting time histories must provide enough information to fully characterize the searched quantity of interest; for this purpose, their length, their precision, and their sampling rate need to meet some minimal requirements.

When the source of the signals is linear, one pursues the identification of the spectral peaks in the Fourier transformation of the signals. The Fourier spectrum is an invariant of the system motion. Only the power associated with the peaks depends on the intensity of the external forcing. When the non-linear features are instead predominant, the two major tools of signals analysis are the fractal dimension and the Lyapunov exponents. They both are invariant during the system evolution, and, hence, they are independent of the changes in the initial conditions and of the co-ordinate system of observation [8]. The fractal dimension and the Lyapunov exponents are linked the one with the others, and hence reference to both of them is done.

This paper discusses the potential of using these quantities to compare multivariate, non-linear time series for the purpose of damage detection and localization, as suggested in References [7, 9]. In particular, the next section provides the governing relations, the subsequent one shows the SHM strategy, and, at last, the proposed methodology is validated by applying it to an experimental case of study whose conditions mirror the reality. The considered structure is the model of the entrance of an ancient noble palace, which is actually located in Palermo, Italy. The specimen was constructed and tested at the ELSA laboratory of the European Union Joint Research Center in Ispra [10].

2. GOVERNING RELATIONS

The Lyapunov exponents were first introduced by Khasminkii [11] when dealing with the stability of stochastic linear systems. Their multiplicative ergodicity was successively proven by the Osedelec theorem [12]. Ergodicity either means that they assume the same values for almost any choice of the initial conditions, in a deterministic context; or that their expected values across the population coincide with their time averages, in a probabilistic context.

The multiplicative ergodicity theorem ensures that the limit by which the Lyapunov exponents are defined (see Equation (4)) exists and is unique. Despite the Lyapunov exponent

concept holds in both a deterministic (chaotic) and stochastic environment [13], their definition is generally introduced in different ways for the two cases. A unifying approach was found in Reference [14].

2.1. Definition of the Lyapunov exponents

Let $\mathbf{x}$ be the vector of the state-variables, of size $n = l-1 = 2h$. The dynamics of the system can be represented by the mapping

$$\mathbf{x}_{j+1} = \mathbf{F}(\mathbf{x}_j) \tag{1}$$

where $\mathbf{F}$ is the system operator evolving along the sequence of time steps represented by index j. Introducing, in the n-dimensional space, a nearby trajectory $\mathbf{y}_j$, the evolution in time of the distance between the two trajectories is

$$\mathbf{y}_{j+1} - \mathbf{x}_{j+1} = \mathbf{F}(\mathbf{y}_j) - \mathbf{F}(\mathbf{x}_j) = \mathbf{J}_j(\mathbf{x}_j)(\mathbf{y}_j - \mathbf{x}_j) + \mathbf{o}(\|\mathbf{y}_j - \mathbf{x}_j\|^2) \tag{2}$$

In Equation (2), $\mathbf{J}_j(\mathbf{x}_j)$ is the n by n Jacobian matrix of $\mathbf{F}$ at $\mathbf{x}_j$, being $\mathbf{F}(\mathbf{y}_j)$ expanded in a Taylor series around $\mathbf{x}_j$. Let us now consider a sequence of N time steps, and build the matrix of the products of the subsequent Jacobian matrices. The ith eigenvalue, $\Lambda_i^{(N)}$, of this matrix can be found from the relationship

$$\prod_{j=1}^{N} \mathbf{J}_j \mathbf{u}_i^{(N)} = \Lambda_i^{(N)} \mathbf{u}_i^{(N)} \tag{3}$$

with $\mathbf{u}_i^{(N)}$ a suitable vector of ortho-normal bases.

The corresponding Lyapunov exponent, λ_i, is then defined as the normalized logarithm of the modulus of the ith eigenvalue, $\Lambda_i^{(N)}$, in the limit of an infinitely long trajectory

$$\lambda_i = \lim_{N\to\infty} \frac{1}{N} \ln |\Lambda_i^{(N)}| \tag{4}$$

The total set of n different exponents is called the Lyapunov spectrum. Their existence and uniqueness is enforced by the Osedelec theorem. They are an invariant measure and remain invariant also for smooth transformation of the state-space.

It is worth noting that, despite the Lyapunov exponents are usually associated with chaotic or stochastic dynamic systems, neither the former nor the latter feature is actually required to compute such an invariant spectrum: the availability of a time series is the only pre-requisite. If the amount of available information is less than the number n of the desired unknown quantities (for instance it is organized in a vector of length N or in a matrix N by ρ, with $\rho < n$), then an embedding dimension $m \geqslant 1$ (equal to the upper integer of the ratio n/ρ) must be introduced to describe a reduced state-space.

Working with a multi-channel data collector, one can assume '*a priori*' and check '*a posteriori*' that the acquired information is overwhelming, and therefore $m = 1$.

2.2. Computation of the Lyapunov exponents

The numerical evaluation of the Lyapunov exponents was first pioneered in Reference [15]. However, it is only with the contribution illustrated in Reference [16] that a standard computation procedure was assessed, leading to the development of the general purpose software of non-linear time series analysis described in Reference [17]. In synthesis, an essential

feature is the estimate of the local Jacobians **J**, i.e. of the linearized dynamics which governs the growth of infinitesimal perturbations. This can be achieved by either of the two following methods:

(i) The first method uses the direct fits of local linear models. Let $\mathbf{s}_j$ the co-ordinates of a point in the working space at the jth time and s_{j+1} the evolution of one of these co-ordinates at next time step. A local linear model is of the type: $s_{j+1} = \mathbf{a}_j \mathbf{s}_j + b_j$. The vector $\mathbf{a}_j$ and the scalar b_j are given by the least squares minimization of the set of vectors $\{\mathbf{s}_s\}_j$ which form the neighbourhood of $\mathbf{s}_j$ [17] and which can be found in the available data. The average of their distance from the starting point will be referred as 'average neighbour size'. The Jacobian matrix collects $\mathbf{a}_j$ as a row vector. When the embedding dimension m is greater than 1, this row is followed by blocks of entries $\delta_{i-1,j}$ for $i = 2, \ldots, m$, with δ denoting the Kroneker index. Of course, the process fails when the minimum number of neighbours cannot be found within the available data.
(ii) As an alternative, one can construct a global non-linear model and compute its local Jacobians by taking the derivatives.

In both cases, the obtained local Jacobians are multiplied one by one, following the trajectory, by as many different vectors $\mathbf{u}_i$ in the tangent space (Equation (3)), as the number of Lyapunov exponents that needs to be computed. Every few steps, a Gram–Schmidt ortho-normalization procedure is applied to the set of $\mathbf{u}_i$, and the logarithms of their rescaling factors are cumulated. Their average, in the order of the Gram–Schmidt procedure, gives the Lyapunov exponents in descending order.

The routine '`lyap_spec`', available in the software package TISEAN 2.1 [17], applies the method of local linear fits. The user must provide as inputs the number of columns, n, of the multivariate time series to be read, and the embedding dimension, m. Then, the routine determines the m by n Lyapunov exponents. In the applications within this paper, it is always $m = 1$.

2.3. Related invariant measures

The knowledge of the Lyapunov exponent spectrum allows one to also compute the following other invariant terms:

(1) According to Pesin's inequality, an upper-bound for the Kolmogorov entropy is given by the sum of all the positive Lyapunov exponents.
(2) The Lyapunov, or Kaplan-Yorke, dimension is defined by the expression

$$D_L = k - \frac{\sum_{i=1}^{k} \lambda_i}{\lambda_{k+1}} \tag{5}$$

where k is the order number of the last Lyapunov exponent (in decreasing order) for which the numerator sum is positive. Roughly speaking, it is the minimal fractal dimension of the space where the dynamics is preserved. Therefore, the assumption $m = 1$ is satisfied when the number of available time histories is greater than D_L. The values of the Lyapunov dimension are directly computed by the routine '`lyap_spec`'.

3. STRATEGY FOR DAMAGE DETECTION AND LOCALIZATION

As a first practical example, the invariant quantities introduced in the previous section are computed from the time series which were recorded during an experiment carried out at the ELSA laboratory of the Joint Research Centre in Ispra. The tested specimen, referred to as a 'baby-frame', is detailed in Reference [7], and the same data were already used for damage detection and localization via a different technique [18, 19]. The structure is excited by repeated shaker pulses and its response is monitored by 18 sensors; the first of them measures the excitation. The collected data form a multi-channel response time histories matrix of 50 000 rows (the sampled points) and 17 columns (the response sensors). Figure 1 shows the first 7500 points of the last column, in the two cases of undamaged and damaged structure; the latter one corresponds to the signal showing higher peaks.

3.1. Damage detection

The direct computation of the Lyapunov exponents and Lyapunov dimension provides the results in the first two rows of Table I. From a visual inspection of Figure 1, the following observations can be argued

(1) The stationarity assumption is not satisfied. Indeed, one could pursue the asymptotic stationarity emphasized in the introduction, but this would require a significant number of shaker pulses and a huge amount of points to be considered in the time series.
(2) Between each couple of successive shaker pulses there is a sequence of 2000 points that corresponds to the period of time during which the external excitation is not active.
(3) Several stationary sequences of the type in (2) could be assembled to form a longer time history.

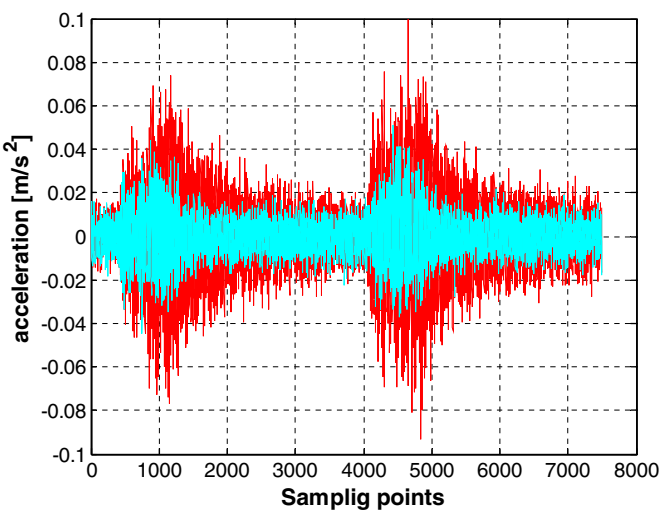

Figure 1. Sensor 18. Measurements of the damaged (signal with higher peaks) and undamaged configurations of the 'baby-frame' specimen described in Reference [7]. Only the first 7500 points are drawn.

Table I. Positive Lyapunov exponents and Lyapunov dimension from the time series recorded during the 'baby-frame' test.

Iterations	Positive Lyapunov exponents							Average neighbour	Lyapunov dimension	Case
First 7500 *rows* (*Figure* 1)										
7499	0.528	0.434	0.336	0.253	0.158	0.084	0.13	0.112	13.062	Undam.
7499	0.434	0.356	0.283	0.208	0.132	0.059		0.104	12.186	Damaged
Six sequences of 2000 *points* (*rows*) *between successive shaker pulses*										
1999	0.372	0.303	0.225	0.162	0.097	0.024		0.020	11.498	Undam.
1999	0.330	0.274	0.210	0.154	0.076			0.017	10.796	Damaged
1999	0.384	0.316	0.236	0.165	0.099	0.039		0.022	11.612	Undam.
1999	0.340	0.270	0.206	0.150	0.083	0.007		0.020	10.825	Damaged
1999	0.365	0.289	0.229	0.156	0.086	0.013		0.026	11.211	Undam.
1999	0.339	0.269	0.209	0.138	0.074			0.021	10.892	Damaged
1999	0.379	0.297	0.234	0.161	0.100	0.026		0.024	11.471	Undam.
1999	0.340	0.275	0.202	0.136	0.072			0.022	10.717	Damaged
1999	0.374	0.309	0.234	0.169	0.105	0.030		0.028	11.479	Undam.
1999	0.333	0.269	0.196	0.138	0.075			0.020	10.745	Damaged
1999	0.368	0.304	0.233	0.165	0.092	0.030		0.022	11.340	Undam.
1999	0.333	0.278	0.205	0.143	0.079			0.022	10.871	Damaged
Two of the six sequences of 2000 *points* (*rows*) *between successive shaker pulses all together*										
3999	0.400	0.336	0.262	0.199	0.134	0.062		0.019	12.209	Undam.
3999	0.383	0.315	0.245	0.175	0.107	0.044		0.018	11.658	Damaged
Three of the six sequences of 2000 *points* (*rows*) *between successive shaker pulses all together*										
5949	0.421	0.353	0.281	0.207	0.139	0.073	0.005	0.021	12.495	Undam.
5949	0.406	0.334	0.255	0.192	0.127	0.061		0.017	12.080	Damaged
Four of the six sequences of 2000 *points* (*rows*) *between successive shaker pulses all together*										
First four sequences										
7999	0.439	0.366	0.296	0.223	0.155	0.090	0.019	0.020	12.843	Undam.
7999	0.414	0.348	0.275	0.211	0.140	0.068		0.017	12.345	Damaged
Last four sequences										
7999	0.448	0.369	0.301	0.232	0.157	0.088	0.016	0.022	12.886	Undam.
7999	0.412	0.339	0.268	0.206	0.139	0.068		0.017	12.271	Damaged
Five of the six sequences of 2000 *points* (*rows*) *between successive shaker pulses all together*										
9949	0.450	0.372	0.303	0.235	0.164	0.100	0.023	0.021	13.033	Undam.
9949	0.423	0.356	0.286	0.217	0.148	0.077	0.005	0.017	12.504	Damaged
All the six sequences of 2000 *points* (*rows*) *between successive shaker pulses together*										
11 949	0.455	0.383	0.309	0.238	0.168	0.104	0.031	0.020	13.134	Undam.
11 949	0.439	0.363	0.298	0.230	0.161	0.087	0.018	0.016	12.745	Damaged

Therefore, the same analysis is repeated for each of the six time series obtained by extracting the stationary sequence between each couple of successive shaker pulses; and for the time series of gradually increasing length formed by assembling different combinations of the previous 2000-points sequences. The results are again in Table I.

One realizes that the numerical values obtained from the six different time series of 2000 points only present small fluctuations (arising from the Lyapunov exponent randomness) among each others, that the average neighbour size (which is here assumed as a measure of accuracy) is nearly the same in all these calculations, and that, in any comparison between damaged and undamaged cases, the numerical values highlight a model modification by discrepancies larger than the intrinsic fluctuations. This is well perceived by the Lyapunov dimension, which is a scalar measure of the higher Lyapunov exponents. Therefore, attention is only focused on the values of the positive Lyapunov exponents, which determine the Lyapunov dimension. Their values are those provided in the tables.

As the length N of the assembled time series increases, there is a sort of (slow) convergence of the limit in Equation (4) to the computed value of the corresponding Lyapunov exponent, and the Lyapunov dimension can be adopted again as the scalar on which the convergence is checked.

The values obtained from these computations are instead quite different from those reported at the end of the first two analyses which included the excitation effects (note that in that case, the average neighbour size is much higher). However, in all the cases, the model difference is always detected by the comparison of the results from the damaged and undamaged situations.

The further computations which led to the results reported in Table II were conducted with the goal of investigating some further properties.

- Scaling the time series by a multiplicative constant (two, in the example) does not change the Lyapunov invariants; one only detects that the average neighbour size results multiplied by the same constant. The numerical example is carried out on the first sequence of 2000 points.

Table II. Further analyses of the 'baby-frame' time series.

Iterations	Positive Lyapunov exponents							Average neighbour	Lyapunov dimension	Case
First sequences of 2000 *points between successive shaker pulses*: *original data* (*from Table* I)										
1999	0.372	0.303	0.225	0.162	0.097	0.024		0.020	11.498	Undam.
1999	0.330	0.274	0.210	0.154	0.076			0.017	10.796	Damaged
First sequences of 2000 *points*: *original data multiplied by* 2										
1999	0.372	0.303	0.225	0.162	0.097	0.024		0.040	11.498	Undam.
1999	0.330	0.274	0.210	0.154	0.076			0.034	10.796	Damaged
First sequences of 2000 *points*: *only the first of each sequential couple of points is retained*										
999	0.328	0.249	0.187	0.129	0.073	0.010		0.023	10.730	Undam.
999	0.327	0.273	0.202	0.131	0.062			0.019	10.548	Damaged
Time series obtained as the assemblage of three sequences of 2000 *points each*: *original data* (*from Table* I)										
5949	0.421	0.353	0.281	0.207	0.139	0.073	0.005	0.021	12.495	Undam.
5949	0.406	0.334	0.255	0.192	0.127	0.061		0.017	12.080	Damaged
Sequence of 12 000 *points*: *only the first of each sequential couple of points is retained* (*time step multiplied by* 2)										
5949	0.436	0.355	0.293	0.219	0.149	0.082	0.010	0.022	12.649	Undam.
5949	0.446	0.372	0.304	0.237	0.158	0.085	0.008	0.017	12.659	Damaged

- Using time histories acquired with different sampling rates could result misleading. Let us consider again the sequence of 2000 points and let us retain only the first of each sequential couple of rows. It means that the time step is multiplied by 2.
- Furthermore, one also investigates the sequence assembled to have 12 000 rows, but retaining only the first of each sequential couple of rows. Since the values are strongly dependent on the iteration number, one compares the results with the ones achieved with a sequence of 6000 rows. The dependence of the results on the time step is evident from the values shown in the last four rows of Table II.

The features observed in this sections allow to formulate the strategy by which the Lyapunov exponents can be used for damage detection.

(a) Several multi-channel time series are directly measured or assembled in such a way that the measurement noise and the external noise can be regarded as stationary.
(b) Among the available time series, the records collected in the undamaged situation must be available and marked as reference case.
(c) The same sampling rate is required.
(d) Subsets of the time series of different lengths are analysed to check the convergence of the procedure.
(e) At each step, the Lyapunov exponents and dimension of the time series which need to be classified as damaged or undamaged, are compared with the results achieved from the time series of the undamaged state.
(f) Damage is detected by identifying a modification in the model invariants.

It must be emphasized that the modification could be masked by special structural features combined with the specific (unsuitable) distribution of sensors.

3.2. Damage localization

Always with reference to the 'baby-frame' test, Table III shows the results obtained by considering a reduced set of channels. In particular, two clusters of four sensors each are separately removed. In one case four sensors faraway from the damage are deleted, so that a model change between the damaged and undamaged situations can still be detected. The second cluster collects, instead, the four sensors which were located all around the damaged region, so that its removal takes away also the damage information and makes the two models not

Table III. Positive Lyapunov exponents and Lyapunov dimension obtained by removing a set of channels from the time series recorded during the 'baby-frame' test.

Iterations	Positive Lyapunov exponents				Average neighbour	Lyapunov dimension	Case
Four sequences of 2000 *points* (*rows*) *& four sensors* (*columns*) *faraway from the damaged area are removed*							
11949	0.310	0.239	0.162	0.078	0.019	8.417	Undamaged
11949	0.280	0.207	0.135	0.051	0.014	7.896	Damaged
Four sequences of 2000 *points* (*rows*) *& four sensors* (*columns*) *all around the damaged area are removed*							
11949	0.278	0.204	0.134	0.055	0.017	8.005	Undamaged
11949	0.267	0.197	0.121	0.042	0.014	7.732	Damaged

anymore distinguishable one from the other. In both cases, the Lyapunov dimension decreases, because information is lost. However, the following remarks allow one to detect when the removed sensors are associated to damage locations:

- When the columns of sensors faraway from the damage are removed from the time series matrices, the models difference stays evident, in the sense that the Lyapunov exponents and dimension computed from the damaged and undamaged cases are still significantly different.
- Removing from the time series the columns of sensors close to the damage also removes the models difference, in the sense that the Lyapunov exponents and dimension on the damaged and undamaged case are close to each other.

The resulting strategy for damage localization is therefore summarized in the following steps:

(a) One starts by removing, one by one, the columns of the two multi-channel time series matrices to be compared (with one of them belonging to the set of the *a priori* identified undamaged signals collection).
(b) If the model difference is still detectable in every situation, one proceeds by removing each couple of columns and by repeating the analysis for these reduced time series.
(c) The process continues until a situation of no model difference is identified. The columns which were removed as last are the signals recorded by the sensors which are located in the proximity of the damaged area(s).

It is worth noting that such a strategy is based on a comparison of relative responses: when locally unchanged, they outline the absence of damage. Special structural configurations, however, could oblige to localize the damage from the separate identification of different areas with no damage. A global study on all these areas could still results in relative modifications when the damaged area is filtering the mutual interaction.

4. VALIDATION OF THE METHOD ON THE 'PALAZZO GERACI FACADE' MODEL

To perform a seismic retrofit study, the façade of an ancient noble palace in Palermo, Sicily, was reproduced by constructing a 1:2 scale masonry specimen. The cracks caused by a series of pseudo-dynamic tests were filled by mortar injections. Measurements of the dynamic response of the structure were taken before and after the repair, by using different excitation methods.

The current state of the structure (after the repair) is shown in Figure 2, and we will refer to it as undamaged. The wall is 8 m wide, 4.6 m high, and 0.7 m thick, and it includes five openings: the central arch and the four lateral ones. Two columns support a frame in front of the arch. Each column is expected to vibrate independently under dynamic loading, and therefore it should be analysed separately. However, this is beyond the scope of the present study, which will neglect the frame motion.

Figure 2 gives evidence of the repaired damage, which mainly affected the right side of the structure. In particular, the feet of the specimen presented the main cracks after the first series of pseudo-dynamic tests. They were therefore strengthened by adding steel brackets at different levels. The confinement effects moved the damage induced by the successive tests to the upper part of the structure, in correspondence to the openings.

The available sensors (Figure 2) monitor the accelerations in the direction parallel to the plane of the façade. Odd numbers are used to identify the sensors located on the right side of the

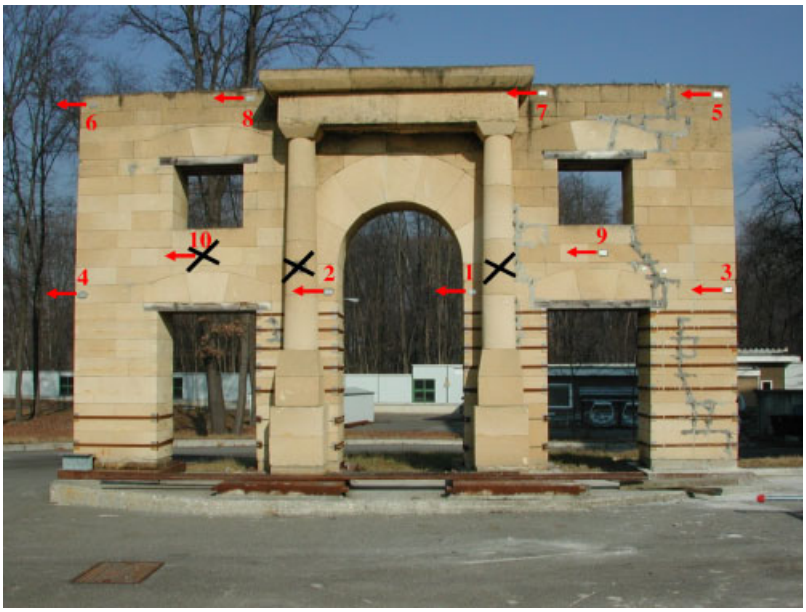

Figure 2. Undamaged state of the Geraci façade specimen, after the retrofit by mortar injections.

specimen. Note that sensor 2 is the only sensor close to a repaired crack in the left side of the structure. Unfortunately, sensor 10 was not working during the tests on the undamaged structure, and it is therefore useless for the purpose of a comparison. Hence, the total number of sensors considered in the analyses is equal to nine.

4.1. Environmental vibration tests

The specimen is currently located outside of the ELSA laboratory of the EU Joint Research Centre in Ispra, Varese. Therefore, it undergoes environmental excitations, such as wind loading and traffic. Its response was measured before and after the cracks repair by performing several environmental vibration tests. The response time histories recorded during two of these tests are selected to compare the damaged (before the repair) and the undamaged (after the repair) states of the structure by the computation of the Lyapunov exponents. Each signal collects a total of 60 000 points (Figure 3). Eight windows of 7500 points each are extracted from every signal and analysed in terms of the previously introduced global measures.

Figure 3 shows, as an example, the accelerations values measured by sensor 5 during the two tests on the damaged and undamaged structure, respectively. The higher peaks recorded during the test on the cracked specimen, suggest that a stronger wind was blowing in that day. To obtain reliable results, one should consider the most homogeneous signal window, i.e. the one which presents the least number of peaks. However, also the windows containing peaks were analysed, and they showed an agreement with the other results, once that the main peaks were removed, thus restoring the stationarity hypothesis.

An attempt to compute the Lyapunov exponents and dimension from the same data was already made in References [7, 9], and the obtained results are reported in the first two rows of Table IV for comparison. It may be noticed that these values refer to the sixth signal window,

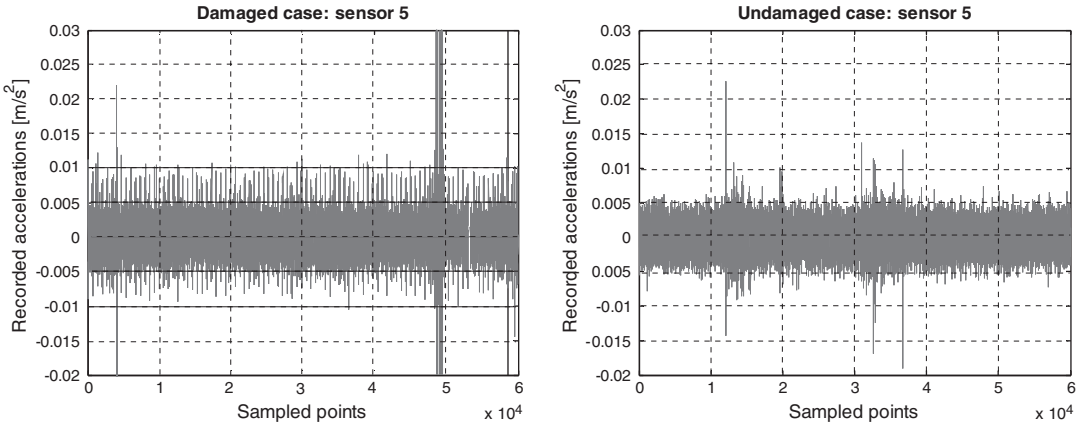

Figure 3. Sensor 5 measurements of: (a) the damaged, i.e. before retrofit; and (b) the undamaged, i.e. after retrofit, configurations of the Geraci specimen described in Reference [7]. 60 000 points were collected during each test.

Table IV. Positive Lyapunov exponents and Lyapunov dimensions computed from the time series recorded during the 'Geraci facade' tests with ambient excitation.

Iterations	Positive Lyapunov exponents			Average neighbour	Lyapunov dimension	Case
Data window 6 *of* 7500 *points* (*rows*) *and* 10 *columns of sensors*						
7499	0.223	0.133	0.033	0.003	5.378	Undamaged
7499	0.222	0.112	0.007	0.007	4.987	Damaged
Data window 6 *of* 7500 *points* (*rows*) *and nine columns of sensors*						
7499	0.158	0.063		0.003	4.052	Undamaged
7499	0.193	0.077		0.007	4.168	Damaged
Data window 4 *of* 7500 *points* (*rows*) *and nine columns of sensors*						
7499	0.153	0.060		0.003	4.039	Undamaged
7499	0.181	0.072		0.005	4.052	Damaged

The column corresponding to sensor 10 is removed in all cases except for the first two rows, which provide a comparison with the previously obtained results.

and that all the 10 sensors were considered in the analyses. Indeed, although sensor 10 was recognized as not working properly, its measurements were kept anyway as the last column of the global time series matrices. In this case, the positive values of the Lyapunov exponents in the two damaged and undamaged situations are only slightly different between each others, with this difference being evident only for the smallest values. Therefore, damage was detected but the results were not sufficiently clear to proceed in its localization.

The analyses are repeated in this study by excluding sensor 10. The resulting global time series matrices have 7500 rows and nine columns instead of 10, being the last one removed. At first, window 6 was analysed to be able to compare the results with the previously obtained ones. The difference between the positive Lyapunov exponents in the damaged and undamaged cases, respectively, becomes significant also for the highest values. However, the average

neighbourhood size also differs between the two cases, thus denoting a relevant non-stationarity. In particular, the highest value is found in the damaged case, which presents the greatest peak intensities. This aspect was checked also for the other signal windows, and it was found that the values of the average neighbourhood size are greatly influenced by the presence of peaks. For example, very high values were obtained from the seventh window of the signals recorded on the damaged structure. However, the value in the undamaged case becomes higher than the other one when the window 5, where the undamaged signals show peaks, is considered.

Therefore, the attention is now shifted on the data window 4, which appears to be the most homogeneous, i.e. with the least number of peaks. The corresponding values of the average neighbourhood size are still different for the damaged and undamaged case, but they are now fairly similar to each other.

The results in Table IV confirm that the positive Lyapunov exponents computed from the time series of the damaged structure, are greater than the ones obtained for the undamaged case. Hence, the damage is successfully detected and we can proceed to its localization.

As suggested by the observations made in the previous section, damage can be localized by removing an increasing number of columns from the global time series matrices associated with the damaged and undamaged cases, until the difference between the two models is not anymore detectable. This situation is reached when the columns corresponding to sensors 2, 3, 5, 7, and 9 are removed, while a model change is still detectable for any other combination of the removed sensors. We recall that sensor 2 is the only accelerometer close to a repaired crack in the left side of the structure. The remaining, identified odd sensors are located close to the main concentrations of damage (cracks), in the right side of the structure. Therefore, it can be concluded that the proposed methodology is also efficient in localizing damage from environmental measurements of non-linear cracked structures, as long as the peak non-stationarities are extracted from the signals (Table V).

4.2. Tests with the hammer

Other series of tests were carried out by inferring hammer strokes to the structure at its two edges, i.e. in proximity of sensor 3, which is located at the middle edge of its right-hand side, and near sensor 4 at the middle edge of the left-hand side, respectively. As already emphasized in

Table V. Positive Lyapunov exponents and Lyapunov dimensions computed from the time series recorded during the 'Geraci facade' tests, with ambient excitation.

Iterations	Positive Lyapunov exponents		Average neighbour	Lyapunov dimension	Case
Data window 4 *of* 7500 *points* (*rows*) *and five columns of sensors not sensitive to the damage* (1, 4, 6, 7, 8) *are removed*					
7499	0.256	0.036	0.0014	2.972	Undamaged
7499	0.241	0.004	0.0023	2.668	Damaged
Data window 4 *of* 7500 *points* (*rows*) *and five columns of sensors sensitive to the damage* (2, 3, 5, 7, 9) *are removed*					
7499	0.223	0.005	0.0013	2.746	Undamaged
7499	0.222	−0.005	0.0012	2.601	Damaged

The multi-channel time series matrices were modified by removing columns of sensors.

Reference [7], the distance of the sensors from the excitation source becomes relevant when perturbing the structural model with a hammer. Indeed, the sensors close to the impact location provide not reliable measurements, because of the much higher intensities with respect to the other sensors time series. In Reference [7], a successful damage analysis was achieved by excluding from the analyses the sensors situated next to the hammer position. Since the records from sensor 10 are meaningless for the undamaged specimen, only the tests with the hammer acting on the left edge of the structure (sensor 4) are considered in the present study. The total number of sensors available for these analyses decreases to seven, and the retained sensors are $1, 2, 3, 5, 7, 8$ and 9. Hence, a spectrum of seven Lyapunov exponents is computed.

The hammer strokes occur at random times and their non-stationary effect needs to be removed from the time histories. After extracting the peaks from both the undamaged and damaged data, several signal windows of 7500 points each were isolated. Table VI provides the positive values of the Lyapunov exponents obtained from the data windows 2 and 5, for both the undamaged and the damaged cases. The structural modification is clearly detected, and the highest values are found from the data collected on the damaged structure.

Table VII synthesizes the outcome of the damage localization procedure. The results achievable from the retained sensors still depend on their distance from the excitation source.

Table VI. Positive Lyapunov exponents and Lyapunov dimensions computed from the time series recorded during the 'Geraci Palace' tests, with hammer excitation near the location of sensor 4.

Iterations	Positive Lyapunov exponents		Average neighbour	Lyapunov dimension	Case
Data window 2 *of* 7500 *points* (*rows*) *and seven columns of sensors*					
7499	0.119	0.007	0.0033	2.921	Undamaged
7499	0.189	0.038	0.0029	3.371	Damaged
Data window 5 *of* 7500 *points* (*rows*) *and seven columns of sensors*					
7499	0.107		0.0023	2.644	Undamaged
7499	0.203	0.052	0.0024	3.471	Damaged

The multi-channel time series matrices do not include the columns corresponding to the sensors situated next to the hammer position. Furthermore, sensor 10 is not considered.

Table VII. Positive Lyapunov exponents and Lyapunov dimensions computed from the time series recorded during the 'Geraci Palace' test, with hammer excitation near sensor 4.

Iterations	Positive Lyapunov exponents		Average neighbour	Lyapunov dimension	Case
Data window 2 *of* 7500 *points* (*rows*) *and three columns of sensors not sensitive to the damage* $(1, 5, 8)$ *are removed*					
7499	0.302	0.052	0.017	3.048	Undamaged
7499	0.223	0.012	0.016	2.741	Damaged
Data window 2 *of* 7500 *points* (*rows*) *and three columns of sensors sensitive to the damage* $(2, 7, 9)$ *are removed*					
7499	0.263	0.026	0.0016	2.860	Undamaged
7499	0.273	0.035	0.0017	2.925	Damaged

The multi-channel time series matrices were modified by removing columns.

Therefore, the measurements from sensors 3 and 5 are in this case not sensitive to the damage, because they are located at the opposite edge with respect to the hammer impact. Sensors 7 and 9, centrally located in the right side of the structure, are instead sensitive to the nearby damage. Sensor 2 is again correctly identified as the only sensor on the left side of the structure to be positioned close to a repaired crack. In conclusion, the localization of cracks from the measurements taken with a hammer is still possible, within the limitations imposed by this excitation technique.

4.3. Final remarks

Although it was computed for all the considered cases, the Lyapunov dimension revealed itself not to be as useful as the positive Lyapunov exponents in detecting and localizing the damage. Its slight modifications between the damaged and undamaged situations do not allow to draw clear conclusions about the state of the structure. However, this dimension is needed to check if the amount of information is sufficient for the problem under consideration.

It may also be noticed that, in this section, damage is detected by an increase of the positive values of the Lyapunov exponents, while the previous results from the 'baby-frame' structure showed a decrease of these values in presence of damage. Once that the undamaged data are available as reference case, the damage identification is however possible by observing a positive or negative model modification. This suggests to introduce, as damage index, the absolute value of the difference between the positive Lyapunov exponents associated with the damaged and undamaged situations, respectively. The relationship of this index with the damage intensity needs to be further investigated.

The authors wanted to first explain the reason of the opposite behaviour of the positive Lyapunov exponents values in the two considered cases of study. One observes that also the computed average neighbourhood sizes show the same discrepancy: they decrease in presence of damage for the 'baby-frame' case, while they increase for the cracked 'Geraci façade' specimen. Therefore, the different behaviour depends on the relative intensities of the sampled signals, intensities which of course are altered by the presence of damage.

5. CONCLUSIONS

This paper approaches time series analysis in the framework of non-linearity, where the invariant measures are the Lyapunov exponents and dimension. The assumption is that the stochastic components are a small contamination of an essentially deterministic non-linear process.

The Whitney's embedding theorem ensures that a set of different variables obtained at the same time can form an embedding space. Thus, multi-channel measurements are recorded, i.e. a set of different variables are measured simultaneously for a single time period. The measurements are then repeated along the system lifetime. Of course, such a set of variables must be sufficient for a complete reconstruction of the system state-space.

The Lyapunov exponents are computed over the resulting multivariate time series. They show to be invariant until a damage is detected. The analysis of reduced subsets of the time series can then be performed to localize the damage itself.

ACKNOWLEDGEMENTS

The research summarized in this paper was supported by a grant from the Italian Ministry of Instruction, University and Research (MIUR), within the program PRIN04. The national research is co-ordinated by Professor Luigi Materazzi of the University of Perugia, Italy.

REFERENCES

1. Kantz H, Schreiber T. *Nonlinear Time Series Analysis*. Cambridge University Press: Cambridge, 1997.
2. Reinhall PG, Caughey TK, Storti DW. Order and chaos in a discrete duffing oscillator: integration and numerical integration. *Journal of Applied Mechanics* 1989; **56**:162–167.
3. Farrar CR, Sohn H, Hemez FM, Anderson MC, Bement MT, Cornwell PhJ, Doebling SW, Schultze JF, Lieven N, Robertson AN. *Damage Prognosis*: *Current Status and Future Needs*. Los Alamos Laboratory, New Mexico, LA-14051-MS, July 2003.
4. Basseville M, Abdelghani M, Benveniste A. *Subspace-based Fault Detection and Isolation—Application to Vibration Monitoring*. INRIA, 3299, Rennes, 1997.
5. Van der Auweraer H, Peeters B. International research projection structural health monitoring: an overview. *Structural Health Monitoring* 2003; **2**(4):341–358.
6. Faravelli L, Casciati S. Structural damage detection and localization by response change diagnosis. *Progress in Structural Engineering and Materials* 2004; **6**(2):104–115.
7. Casciati S. Damage detection and localization in the space of the observed variables. *Ph.D. Thesis*, Department of Structural Mechanics, University of Pavia, 2005.
8. Abarbanel HDI. *Analysis of Observed Chaotic Data*. Springer: New York, 1996.
9. Casciati F, Casciati S, Faravelli L. Lyapunov exponents of measured data for damage detection. *Proceedings 9th International Energy Engineering Conference*, Sharm el Sheick, Egypt, CD, 2005.
10. Beni F, Lagomarsino S, Marazzi F, Magonette G, Podestà S. Structural monitoring through dynamic identification. In *Proceedings of the 3rd World Conference on Structural Control*, vol. 3, Casciati F (ed.). Wiley: Chichester, 2003; 139–152.
11. Khasminskii RZ. Necessary and sufficient conditions for almost sure asymptotic stability of linear stochastic systems. *Theory of Probability and Applications* 1967; **12**(1):144–147.
12. Oseledec VI. A multiplicative ergodic theorem, Lyapunov characteristic numbers for dynamical systems. *Transactions of the Moscow Mathematical Society* 1968; **19**:197–231.
13. Wedig WV. Invariant measures and Lyapunov exponents for generalized parameter fluctuations. In *Nonlinear Structural Systems under Random Conditions*, Casciati F, Elishakoff I, Roberts JB (eds). Elsevier: Amsterdam, 1990; 13–25.
14. To CSW, Liu ML. Lyapunov exponents and information dimensions of multi-degree-of-freedom systems under deterministic and stationary random excitations. In *IUTAM Symposium in Advances Stochastic Mechanics*, Naess A, Krenk S (eds). Kluwer Academic Publisher: Dordrecht, 1996; 449–458.
15. Wolf A, Swift JB, Swiney HL, Vasano JA. Determining Lyapunov exponents from a time series. *Physica* 1985; **16D**:285–317.
16. Sano M, Sawada Y. Measurement of the Lyapunov spectrum from a chaotic time series. *Physical Review Letters* 1985; **55**:1082.
17. Hegger R, Kantz K, Screiber T. Practical implementation of nonlinear time series methods: the TISEAN package. *Chaos* 1999; **9**:413–435.
18. Casciati S, Colabrese E, Magonette G. Damage detection and localization by statistical comparison of response time histories. In *Structural Health Monitoring 2003*, Chang F-K (ed.). DEStech: Lancaster, 2003; 733–741.
19. Casciati S, Colabrese E, Magonette G. Monitoring and response surface methodology to detect and locate structural damage. In *Structural Health Monitoring and Intelligent Infrastructures*, Wu Z, Abe M (eds). Balkena: Lisse, 2003; 423–429.

